Journal of information and
communication convergence engineering
http://jicce.org

J. Inf. Commun. Converg. Eng. 14(3): 200-206, Sep. 2016 **Regular paper**

Color Compensation of an Underwater Imaging System Using Electromagnetic Wave Propagation

Kotaro Inoue[1], Min-Chul Lee[1], Cheol-Su Kim[2], and Myungjin Cho[3*], *Member, KIICE*

[1]Department of Computer Science and Electronics, Kyushu Institute of Technology, Fukuoka 820-8502, Japan
[2]Department of Electric Energy and Computer Engineering, Gyeongju University, Gyeongju 38065, Korea
[3]Department of Electrical, Electronic, and Control Engineering, IITC, Hankyong National University, Anseong 17579, Korea

Abstract

Images can be obtained by collecting rays from objects. The characteristics of electromagnetic wave propagation depend on the medium. In particular, in an underwater imaging system, the interface between air and water must be considered. Further, reflection and transmission coefficients can be found by using electromagnetic theory. Because of the fact that the values of these coefficients differ according to the media, the recorded light intensities will change. A color image sensor has three different color channels. Therefore, the reflection and transmission coefficients have to be calculated individually. Thereafter, by using these coefficients, we can compensate for the color information of underwater objects. In this paper, we present a method to compensate for the color information of underwater objects by using electromagnetic wave propagation theory. To prove our method, we conducted optical experiments and evaluated the quality of the compensated image by a metric known as mean square error.

Index Terms: Color compensation, Integral imaging, Reflection, Refraction, Underwater imaging

I. INTRODUCTION

Imaging of underwater objects has various applications and benefits in the fields of marine sciences, inspection of vessels, security and defense, underwater exploration, unmanned underwater vehicles, etc. [1-5]. There are many optical effects to consider when approaching an in-water imaging situation. Water and the varying particles in it are responsible for numerous effects such as wavelength-dependent absorption, attenuation, scattering, reflection, and the index of refraction variations [5, 6]. Thus, underwater imaging is inherently different from aerial imaging. Absorption and scattering problems may be solved using statistical image processing techniques [7]. However, since other wave propagation parameters in water are caused by the difference in the medium features between in air and in water, the recorded underwater image has some distortions.

In the underwater color imaging case, a color image sensor has three different basic color sensors, namely red (R), green (G), and blue (B). Each color sensor detects light information at a different wavelength (R: 620–750 nm, G: 495–570 nm, and B: 450–475 nm). This means that each channel has different wave propagation parameters. Therefore, we need to consider these differences among basic colors for the acquisition of accurate underwater images. Further, since the refraction index of water is different from that of air, the image magnification should be adjusted.

Received 11 August 2016, **Revised** 13 August 2016, **Accepted** 17 August 2016
***Corresponding Author** Myungjin Cho (E-mail: mjcho@hknu.ac.kr, Tel: +82-31-670-5298)
Department of Electrical, Electronic, and Control Engineering, Hankyong National University, 327 Chungang-ro, Anseong 17579, Korea.

Open Access **http://dx.doi.org/10.6109/jicce.2016.14.3.200** print ISSN: 2234-8255 online ISSN: 2234-8883

In this paper, we describe wave propagation parameters for each color channel by using electromagnetic theory. Then, color compensation is presented. To prove our compensation method, we conduct an optical experiment and evaluate the quality of the results by using mean square error as the metric.

II. MAGNIFICATION OF UNDERWATER IMAGING

At the interface between air and water as shown in Fig. 1, the waves are refracted by Snell's law as per the following equation [8, 9].

$$n_1 \sin\theta_1 = n_2 \sin\theta_2 , \tag{1}$$

where n_1 and n_2 denote the refraction index of medium 1 (air) and medium 2 (water), respectively, and θ_1 and θ_2 represent the incident wave angle and the refraction wave angle, respectively.

According to this law, the underwater objects seem to float. However, since on-axis underwater imaging is used in this study, the range parameter z_{water} as shown in Fig. 1 should be changed as follows [10]:

$$z'_{water} = \frac{z_{water}}{n_2} , \tag{2}$$

where z_{water} denotes the actual distance between the water surface and the objects, and z'_{water} represents the distance between the water surface and the object image as depicted distance is shorter than the actual distance between the in Fig. 1. Therefore, the object image image sensor and the object. To obtain an image with the correct magnification, we need to resize the underwater image by using Eq. (2). The following equation presents the adjusted magnification in water [10].

$$M_{air} = \frac{f}{z_{air} + z_{water}} , \tag{3}$$

$$M_{water} = \frac{f}{z_{air} + z'_{water}} = \frac{f}{z_{air} + z_{water} / n_2} , \tag{4}$$

where f denotes the focal length of the imaging lens and z_{air} represents the distance between the lens and the water surface.

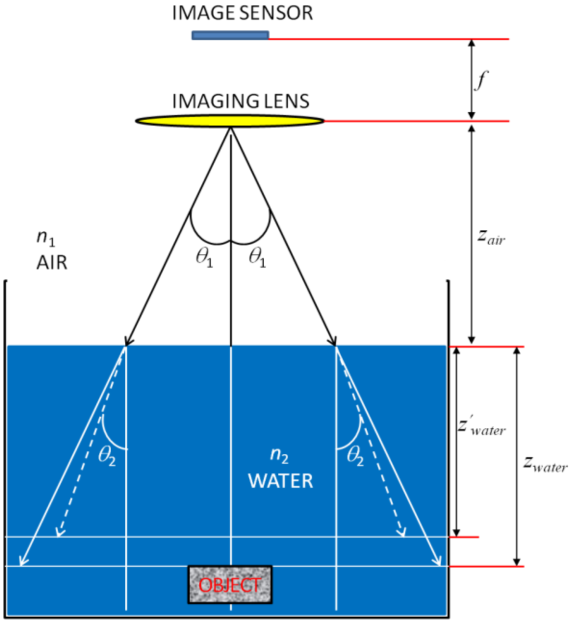

Fig. 1. Underwater imaging with refraction.

III. UNDERWATER IMAGE RECORDING PROCESS

The underwater image recording process has two major steps: illumination and recording. In the illumination step, the illumination wave propagates from air to water. Further, in the recording step, the object wave comes from water to air.

Step 1. Illumination

Fig. 2 illustrates the illumination step. The light bulb emits the incident illumination plane wave. Hereafter, we consider the electric field only for the simplicity of calculation.

As shown in Fig. 2, we have two different media (air and

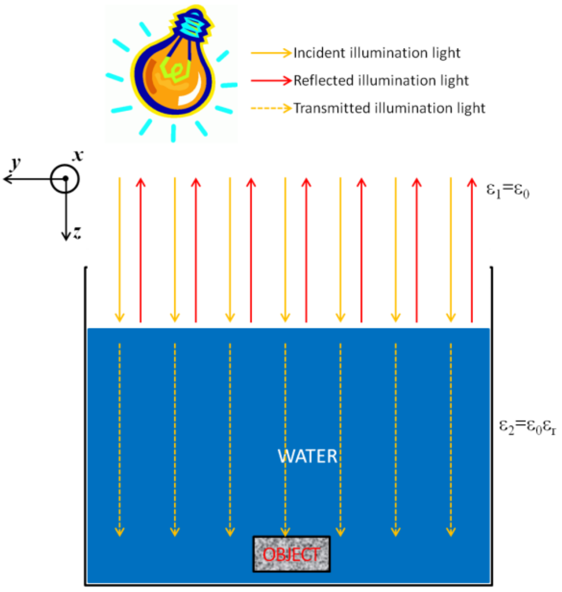

Fig. 2. Illumination step.

water). Therefore, the wave impedance Z_{w1} and Z_{w2} can be calculated by using the following equations [9]:

$$Z_{w1} = \eta_1 = \sqrt{\frac{\mu_0}{\varepsilon_0}} \approx 377\,, \tag{5}$$

$$Z_{w2} = \eta_2 = \sqrt{\frac{\mu_0}{\varepsilon_0 \varepsilon_r}} \approx 377\sqrt{\frac{1}{\varepsilon_r}} = 377 \times \frac{1}{n_2}\,, \tag{6}$$

where μ_0 denotes the magnetic permeability in air, ε_0 indicates the electric permittivity in air, ε_r represents the relative permittivity in the medium, and n_2 refers to the refraction index of medium 2 (water).

The wave impedance Z_{w1} is always constant. On the other hand, Z_{w2} can be changed for each color channel (R, G, and B). The wave impedance for each color channel can be found by using the following equations [9]:

$$Z_{w2}^{R} = \eta_2^{R} = \sqrt{\frac{j\omega_R \mu_0}{j\omega_R \varepsilon_0 \varepsilon_r + \sigma}}\,, \tag{7}$$

$$Z_{w2}^{G} = \eta_2^{G} = \sqrt{\frac{j\omega_G \mu_0}{j\omega_G \varepsilon_0 \varepsilon_r + \sigma}}\,, \tag{8}$$

$$Z_{w2}^{B} = \eta_2^{B} = \sqrt{\frac{j\omega_B \mu_0}{j\omega_B \varepsilon_0 \varepsilon_r + \sigma}}\,, \tag{9}$$

where $\omega_R = 2\omega f_R$, $\omega_G = 2\omega f_G$, $\omega_B = 2\omega f_B$, and σ denotes the conductivity of the medium. However, in this case, we can use the following equation instead of Eqs. (7)–(9) to find the wave impedance of each color channel because of the very low conductivity of water [9].

$$Z_{w2}^{R,G,B} = \eta_2^{R,G,B} = \frac{\eta_0}{n_2^{R,G,B}}\,, \tag{10}$$

where $n_2^{R,G,B}$ denotes the refraction index of each channel.

Now, we know the wave impedance of each color channel. Therefore, we can calculate the reflection and the transmission coefficient for each channel by using the following equations [9]:

$$\Gamma_1^{R} = \frac{\eta_2^{R} - \eta_1}{\eta_2^{R} + \eta_1} = \frac{1/n_2^{R} - 1}{1/n_2^{R} + 1}\,, \tag{11}$$

$$\Gamma_1^{G} = \frac{\eta_2^{G} - \eta_1}{\eta_2^{G} + \eta_1} = \frac{1/n_2^{G} - 1}{1/n_2^{G} + 1}\,, \tag{12}$$

$$\Gamma_1^{B} = \frac{\eta_2^{B} - \eta_1}{\eta_2^{B} + \eta_1} = \frac{1/n_2^{B} - 1}{1/n_2^{B} + 1}\,, \tag{13}$$

$$T_1^{R} = \frac{2\eta_2^{R}}{\eta_1 + \eta_2^{R}} = \frac{2/n_2^{R}}{1 + 1/n_2^{R}}\,, \tag{14}$$

$$T_1^{G} = \frac{2\eta_2^{G}}{\eta_1 + \eta_2^{G}} = \frac{2/n_2^{G}}{1 + 1/n_2^{G}}\,, \tag{15}$$

$$T_1^{B} = \frac{2\eta_2^{B}}{\eta_1 + \eta_2^{B}} = \frac{2/n_2^{B}}{1 + 1/n_2^{B}}\,. \tag{16}$$

To calculate the attenuation coefficient of a medium, we need to figure out $(\sigma/\omega\varepsilon)^2$. In the case of visible light propagation through water, $\omega\varepsilon$ is sufficiently large and σ is very small. Therefore, $(\sigma/\omega\varepsilon)^2$ is set to <<1 so that the medium can be good dielectric [9]. In a good dielectric, the attenuation coefficient α can be defined as follows [9]:

$$\alpha = \frac{\sigma}{2}\sqrt{\frac{\mu_0}{\varepsilon_0 \varepsilon_r}} = \frac{\sigma}{2}\eta_0 \sqrt{\frac{1}{\varepsilon_r}} = \frac{\sigma}{2}\eta_0 \frac{1}{n_2}\,. \tag{17}$$

For each color channel, we can find the attenuation coefficient by using the following equation:

$$\alpha^{R,G,B} = \frac{\sigma}{2n_2^{R,G,B}}\eta_0\,. \tag{18}$$

To find the electric field of the illumination light, we assume that the incident electric field is $E^i = E_0 e^{-j\beta_1 z_{air}}$. Therefore, the reflected electric field and the transmitted electric field of the illumination light can be $E^r = \Gamma_1 E_0 e^{+j\beta_1 z_{air}}$ and $E^t = T_1 E_0 e^{-\alpha z_{water}} e^{-j\beta_2 z_{water}}$.

Step 2. Recording of underwater image

Fig. 3 describes the recording of an underwater image. The transmitted illumination light can be the incident object light in this step. We do not need to consider the reflected object light because it cannot reach the image sensor. Therefore, here, we only consider the transmission coefficient through the air to be as follows [9]:

$$T_2^{R} = \frac{2\eta_1}{\eta_2^{R} + \eta_1} = \frac{2}{1/n_2^{R} + 1}\,, \tag{19}$$

$$T_2^{G} = \frac{2\eta_1}{\eta_2^{G} + \eta_1} = \frac{2}{1/n_2^{G} + 1}\,, \tag{20}$$

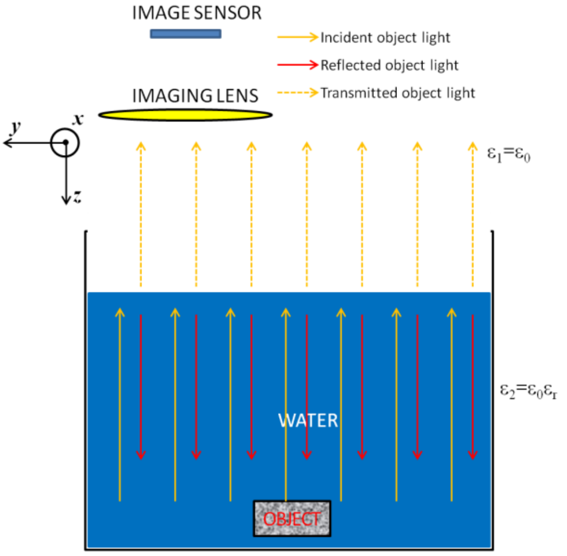

Fig. 3. Recording of an underwater image.

$$T_2^B = \frac{2\eta_1}{\eta_2^B + \eta_1} = \frac{2}{1/n_2^B + 1}. \tag{21}$$

In the air medium, the attenuation coefficient can be ignored because the conductivity of air is almost zero. Thus, the electric fields of the incident and the transmitted object lights can be defined as follows [9]:

$$E^{io} = T_1 \tilde{E}_0 e^{-\alpha z_{water}} e^{+j\beta_2 z_{water}}, \tag{22}$$

$$E^{to} = T_2 T_1 \tilde{E}_0 e^{-\alpha z_{water}} e^{+j\beta_1 z_{air}}, \tag{23}$$

where $\tilde{E}_0 = E_0 E_{obj}$ represents the object light intensity.

Therefore, the total recorded electric field can be calculated as follows:

$$\begin{aligned} E^{tot} &= E^r + E^{to} = \Gamma_1 E_0 e^{+j\beta_1 z_{air}} + T_2 T_1 E_0 E_{obj} e^{-\alpha z_{water}} e^{+j\beta_1 z_{air}} \\ &= \left(\Gamma_1 + T_2 T_1 E_{obj} e^{-\alpha z_{water}}\right) E_0 e^{+j\beta_1 z_{air}} \end{aligned}. \tag{24}$$

IV. COMPENSATION OF EACH COLOR CHANNEL USING ELECTROMAGNETIC THEORY

Thus far, we have calculated the wave propagation parameters in both the illumination and the recording steps. However, our goal is to estimate the original image (in-air image) from the underwater image. Further, the image sensor can detect only the average power of the propagated wave. Therefore, we need to calculate the average power of each step, underwater image, and the original image as follows [9]:

$$S_{av}^r = \frac{1}{2}\mathrm{Re}\left(E^r \times H^{r*}\right) = \frac{1}{2\eta_1}\left|\Gamma_1\right|^2 \left|E_0\right|^2, \tag{25}$$

$$S_{av}^{to} = \frac{1}{2}\mathrm{Re}\left(E^{to} \times H^{to*}\right) = \frac{1}{2\eta_1}\left|T_2\right|^2 \left|T_1\right|^2 \left|E_0\right|^2 \left|E_{obj}\right|^2 e^{-2\alpha z_{water}}, \tag{26}$$

$$S_{av}^{tot} = S_{av}^r + S_{av}^{to} = \frac{1}{2\eta_1}\left|E_0\right|^2 \left(\left|\Gamma_1\right|^2 + \left|T_2\right|^2 \left|T_1\right|^2 \left|E_{obj}\right|^2 e^{-2\alpha z_{water}}\right), \tag{27}$$

$$S_{av}^{ori} = \frac{1}{2\eta_1}\left|E_0\right|^2 \left|E_{obj}\right|^2, \tag{28}$$

where $S^r{}_{av}$, $S^{to}{}_{av}$, $S^{tot}{}_{av}$, and $S^{ori}{}_{av}$ denote the average power of the reflected illumination light, the transmitted object light, the total underwater image light, and the original image light, respectively.

Using Eqs. (25)–(28), we can estimate the original image from the underwater image as follows:

$$\hat{S}_{av}^R = \left(\frac{S_{av}^{tot,R} - S_{av}^{r,R}}{\left|T_2^R\right|^2 \left|T_1^R\right|^2}\right) \times e^{+2\alpha^R z_{water}}, \tag{29}$$

$$\hat{S}_{av}^G = \left(\frac{S_{av}^{tot,G} - S_{av}^{r,G}}{\left|T_2^G\right|^2 \left|T_1^G\right|^2}\right) \times e^{+2\alpha^G z_{water}}, \tag{30}$$

$$\hat{S}_{av}^B = \left(\frac{S_{av}^{tot,B} - S_{av}^{r,B}}{\left|T_2^B\right|^2 \left|T_1^B\right|^2}\right) \times e^{+2\alpha^B z_{water}}. \tag{31}$$

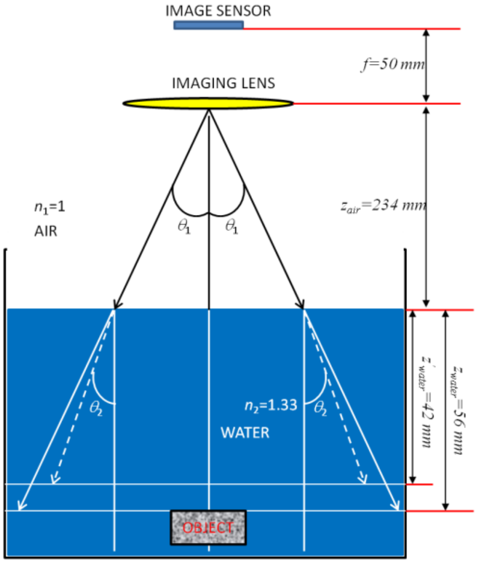

Fig. 4. Diagram of the experimental setup.

V. EXPERIMENTAL RESULTS

To prove our compensation method for an underwater image, we conducted an optical experiment. Fig. 4 shows the experimental setup.

In the optical experiment, a camera with the focal length of $f = 50$ mm is used. It has 2496 (H) × 1664 (V) pixels. The distance between the imaging lens and the water surface, $z_{air} = 234$ mm, the distance between the water surface and the object, $z_{water} = 56$ mm, and the distance between the imaging lens and the object image, $z'_{water} = z_{water}/n_2 = 42$ mm, respectively. Fig. 5 shows the in-air image and the underwater image used in this experiment.

To compare the underwater image with the in-air image, we adjust the magnification of the underwater image by using Eqs. (3) and (4). The experimental images with the adjusted magnification are shown in Fig. 6. Then, we evaluate the quality of the processed image by using mean square error (MSE) as the metric:

$$MSE_{non-processed} = E\left[\left(S_{av}^{ori} - S_{av}^{tot}\right)^2\right], \qquad (32)$$

$$MSE_{processed} = E\left[\left(S_{av}^{ori} - \hat{S}_{av}\right)^2\right]. \qquad (33)$$

MSE in the case of the non-processed image is always constant, $MSE_{non-processed} = 461.86$. However, MSE in the case of the processed image changes with a change in the conductivity of water. Fig. 7 shows the plot of MSE in the cases of the processed image and the non-processed image versus the conductivity of water.


(a) (b)

Fig. 5. Images used in the optical experiment: (a) in-air and (b) underwater.


(a) (b)

Fig. 6. Images with the adjusted magnification: (a) in-air and (b) underwater.

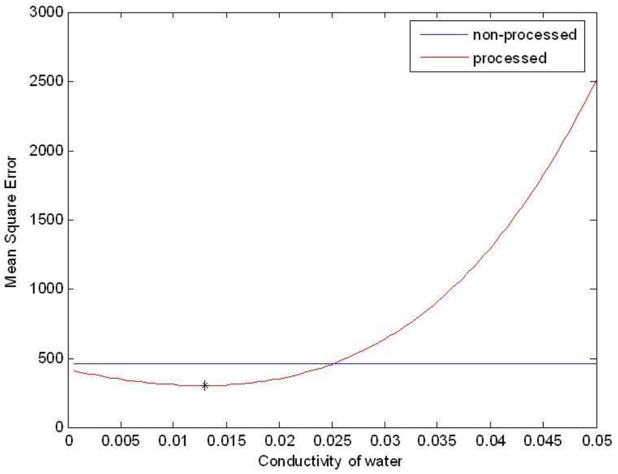

Fig. 7. Plot of MSE in the cases of the non-processed image and the processed image versus the conductivity of water. The optimum conductivity of water is 0.013.

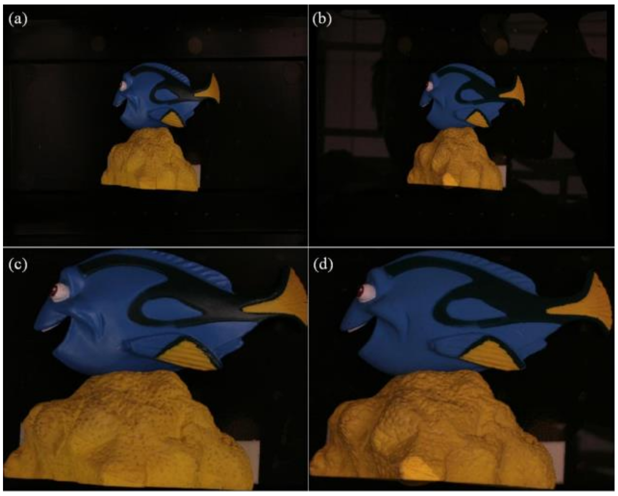

Fig. 8. Experimental results: (a) and (c) show the in-air images with the original scale and the enlarged scale, and (c) and (d) show the color-compensated underwater images with the original scale and the enlarged scale.

As shown in Fig. 7, the best MSE result is obtained at the optimum water conductivity of 0.013. Using this optimum conductivity and Eqs. (29)–(31), we can obtain the color-compensated underwater images as depicted in Fig. 8(b) and (d).

In Fig. 8(c) and (d), the colors yellow and blue have a similar intensity value. Thus, the MSE in the case of the processed image is better than that in the case of the non-processed image.

VI. CONCLUSIONS

In this paper, we present the color compensation method for an underwater imaging system. Using electromagnetic theory, we can find the wave propagation parameters such as the reflection, transmission, and attenuation coefficient of a wave for each basic color channel. Since the image sensor detects only the average power of a wave, we need to calculate the average power of the wave for each color channel. As shown in the experimental results, the color-compensated image is better than the non-processed image. Further, through the optimization process for the conductivity of water, we can find optimum conductivity because we do not know the exact conductivity of water. The range of water conductivity is 5×10^{-4} to 5×10^{-2} S/m. Using optimum conductivity, we can estimate the original image well. Therefore, we can expect underwater object recognition to be implemented well by using this color compensation method.

ACKNOWLEDGMENTS

This research was supported by Basic Science Research Program through the National Research Foundation of Korea (NRF) funded by the Ministry of Education (No. NRF-2015R1A2A1A16074936).

REFERENCES

[1] L. Mullen, A. J. C. Vieira, P. R. Herezfeld, and V. M. Contarino, “Application of RADAR technology to aerial LIDAR systems for enhancement of shallow underwater target detection,” *IEEE Transactions on Microwave Theory and Techniques*, vol. 43, no. 9, pp. 2370-2377, 1995.

[2] F. Okano, J. Arai, H. Hoshino, and I. Yuyama, “Three-dimensional video system based on integral photography,” *Optical Engineering*, vol. 38, no. 6, pp. 1072-1077, 1999.

[3] D. M. Kocak, F. R. Dalgleish, F. M. Caimi, and Y. Y. Schechner, “A focus on recent development and trends in underwater imaging,” *Marine Technology Society Journal*, vol. 42, no. 1, pp. 52-67, 2008.

[4]P. Stand, “Underwater electro-optical system for mine identification,” in *Detection Technologies for Mines and Minelike Targets, Proceedings of the SPIE, vol. 2496*. Bellingham, WA: International Society for Optics and Photonics, pp. 487-497, 1995.

[5] L. E. Mertens, *In-Water Photography: Theory and Practice*. New York: Wiley-Interscience, 1970.

[6] T. Glover, G. E. Harwood, and J. N. Lythgoe, *A Manual of Underwater Photography*. New York: Academic Press, 1977.

[7] M. Cho and B. Javidi, “Three-dimensional visualization of objects in turbid water using integral imaging,” *Journal of Display Technology*, vol. 6, no. 10, pp. 544-547, 2010.

[8] E. Hecht, *Optics*, 4th ed. Reading, MA: Addison-Wesley, 2001.

[9] C. A. Balanis, *Advanced Engineering Electromagnetics*. New York: John Wiley & Sons, 1989.

[10] R. Schulein and B. Javidi, “Underwater multi-view three-dimensional imaging,” *Journal of Display Technology*, vol. 4, no. 4, pp. 351-353, 2008.

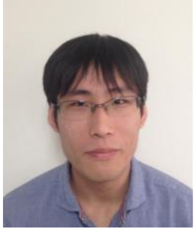

Kotaro Inoue

received his B.S. degree from Kyushu Institute of Technology, Fukuoka, Japan, in 2015. He is a graduate student at Kyushu Institute of Technology, Japan. His research interests include visual feedback control, 3D display, and 3D integral imaging.

Min-Chul Lee

received his B.S. in Telecommunication Engineering from Pukyong National University, Busan, Korea, in 1996, and his M.S. and Ph.D. degrees from Kyushu Institute of Technology, Fukuoka, Japan, in 2000 and 2003, respectively. He is an assistant professor at Kyushu Institute of Technology, Japan. His research interests include medical imaging, blood flow analysis, 3D display, 3D integral imaging, and 3D biomedical imaging.

Cheol-Su Kim
received his B.S., M.S., and Ph.D. in Electronic Engineering from Kyungpook National University, Daegu, Korea, in 1989, 1991, and 1997, respectively. He is currently an associate professor in the Department of Computer and Information Engineering, Gyeongju University. His current research interests include optical memory systems, holography, optical security, and optical signal processing.

Myungjin Cho
received his B.S. and M.S. in Telecommunication Engineering from Pukyong National University, Pusan, Korea, in 2003 and 2005, respectively, and his M.S. and Ph.D. in Electrical and Computer Engineering from University of Connecticut, Storrs, CT, USA, in 2010 and 2011, respectively. Currently, he is an assistant professor at Hankyong National University, Korea. He worked as a researcher at Samsung Electronics, Korea, from 2005 to 2007. His research interests include 3D displays, 3D signal processing, 3D biomedical imaging, 3D photon counting imaging, 3D information security, 3D object tracking, and 3D underwater imaging.